

Prediction of N0 Irradiated Rectal Cancer Comparing MRI Before and After Preoperative Chemoradiotherapy

Fabio Pomerri, M.D.¹ • Filippo Crimi, M.D.¹ • Nicola Veronese, M.D.²
Alessandro Perin, M.D.³ • Carmelo Lacognata, M.D.⁴ • Francesca Bergamo, M.D.⁵
Caterina Boso, M.D.⁶ • Isacco Maretto, M.D.³

1 Department of Medicine, Institute of Radiology, University of Padova, Padova, Italy

2 Department of Medicine, Geriatric Section, University of Padova, Padova, Italy

3 Department of Surgery, Oncology and Gastroenterology, University of Padova, Padova, Italy

4 Department of Radiology, Azienda Ospedaliera of Padova, Padova, Italy

5 Medical Oncology 1, Istituto Oncologico Veneto Istituto di Ricovero e Cura a Carattere Scientifico, Padova, Italy

6 Radiation Oncology, Istituto Oncologico Veneto Istituto di Ricovero e Cura a Carattere Scientifico, Padova, Italy

BACKGROUND: The prediction of lymph node status using MRI has an impact on the management of rectal cancer, both before and after preoperative chemoradiotherapy.

OBJECTIVE: The purpose of this study was to maximize the negative predictive value and sensitivity of mesorectal lymph node imaging after chemoradiotherapy because postchemoradiation node-negative patients may be treated with rectum-sparing approaches.

DESIGN: This was a retrospective study.

SETTINGS: The study was conducted at a tertiary care hospital.

PATIENTS: Sixty-four patients with locally advanced rectal cancer who underwent preoperative chemoradiotherapy and MRI for staging and the assessment of response were evaluated.

MAIN OUTCOME MEASURES: The sums of the sizes of all mesorectal lymph nodes in each patient on both prechemoradiotherapy and postchemoradiotherapy imaging

Funding/Support: This work was partially supported by the Italian Ministry of Health (Progetti Ordinari di Ricerca Finalizzata No. RF-2011-02349645) and by the University of Padova (Progetti di Ateneo, PRAT 2015).

Financial Disclosure: None reported.

Correspondence: Fabio Pomerri, M.D., Department of Medicine, University of Padova, via Giustiniani 2, 35128 Padova, Italy. E-mail: fabio.pomerri@unipd.it

Dis Colon Rectum 2017; 60: 1184–1191

DOI: 10.1097/DCR.0000000000000894

© The ASCRS 2017

data sets were calculated to determine the lymph node global size reduction rates, taking these to be the outcomes of the histopathologic findings. Other included measures were interobserver agreement regarding the prediction of node status based on morphologic criteria and the diagnostic performance of contrast-enhanced images.

RESULTS: Using a cutoff value of a 70% lymph node global size reduction rate with only 15 node-positive patients on histopathology, the sensitivity in the prediction of nodal status and negative predictive value were 93% (95% CI, 70.2%–98.8%) and 97% (95% CI, 82.9%–99.8%) for observer 1 and 100% (95% CI, 79.6%–100%) and 100% (95% CI, 62.9%–100%) for observer 2. The areas under the receiver operating characteristic curves for the 2 observers were 0.90 (95% CI, 0.82–0.98; $p < 0.0001$) for observer 1 and 0.65 (95% CI, 0.50–0.79; $p = 0.08$) for observer 2. The efficacy of the morphologic criteria and contrast-enhanced images in predicting node status was limited after chemoradiotherapy.

LIMITATIONS: This study is limited by its small sample size and retrospective nature.

CONCLUSIONS: Assessing the lymph node global size reduction rate value reduces the risk of undetected nodal metastases and may be helpful in better identifying suitable candidates for the local excision of early stage rectal cancer. See **Video Abstract** at <http://links.lww.com/DCR/A412>.

KEY WORDS: Chemoradiotherapy; Lymph node; Magnetic resonance imaging; Negative predictive value; Rectal cancer; Staging.

Preoperative chemoradiotherapy (pCRT), followed by total mesorectal excision (TME), is the standard of care for patients with midlow locally advanced rectal cancer (LARC).¹ This approach leads to improved local control, with an expected rate of local relapse of 6%.² The use of pCRT induces the downsizing and downstaging of the primary tumor, yielding a pathologic intermediate (ypT1–2N0) or complete response (ypT0N0) in 27% to 29% and 18% to 19% of patients.^{3,4} Because the combined pCRT and TME approach carries a relevant risk of perioperative and postoperative morbidity and may impact negatively health-related quality of life,⁵ rectum-sparing approaches, such as transanal local excision^{6,7} or a wait-and-see policy,⁸ have been proposed as alternative treatments to TME surgery for patients showing a major or complete clinical response after pCRT.

A major concern regarding rectum-sparing approaches is related to the risk of leaving metastatic lymph nodes (LNs) in the mesorectum. This risk is associated with the ypT stage (2.0%–9.1% for ypT0 tumors, 15.0%–17.1% for ypT1 tumors, and 17.0%–20.8% for ypT2 tumors).^{9–11} An accurate assessment of nodal status via MRI therefore plays a key role in the management of rectal cancer after pCRT.

Studies on MRI use for local restaging after pCRT have reported considerable differences in methodologic analysis and results in terms of assessing LN status in both the pre-pCRT and post-pCRT staging of LARC.^{12–16} Individual nodal staging via imaging is mainly based on the use of size, internal signal, and border contour characteristics. It is widely accepted that individual LN size and morphologic criteria are not accurate predictors of nodal status after pCRT and may lead to inaccurate MRI LN restaging.^{17,18} Moreover, most studies in this field have not focused on the negative predictive value (NPV) of staging imaging, which is crucial when a rectum-sparing approach is planned. Our study is based on the hypothesis that the downsizing of mesorectal LNs, as a whole, may predict the LN status after pCRT in LARC.

The primary goal of our retrospective study was to maximize the NPV and sensitivity of MRI for the restaging of local LNs, calculating the sums of the short diameters of all mesorectal LNs in each patient in both the pre-pCRT and post-pCRT MRI data sets to determine the pre-pCRT and post-pCRT LN global sizes and the LN global size reduction rates (Δ LN global size). The secondary goals were interobserver reproducibility assessment and evaluating the usefulness of gadolinium-enhanced MRI sequences in determining LN status after pCRT.

PATIENTS AND METHODS

Patient Selection

The local institutional review board waived informed consent for the retrospective review of clinical patient data.

The inclusion criteria for our study were biopsy-proved midlow (<11 cm from the anal verge) adenocarcinoma of the rectum, TNM clinical stage II or III, an Eastern Cooperative Oncology Group performance status of 0 to 2, and having been treated with pCRT. Patients who did not undergo both pre-pCRT and post-pCRT MRI at our institution were excluded, as were those who did not undergo radical surgery. The workup included a clinical history and physical examination, proctoscopy and colonoscopy, CEA assay, thoracic and abdominal CT, and pelvic MRI. Between January 2009 and November 2015, 140 consecutive patients with LARC underwent pCRT. Of these patients, 63 were excluded because they did not undergo both pre-pCRT and post-pCRT MRI at our institution, and 13 were excluded because they underwent a local excision treatment. The remaining 64 patients formed the study group.

Treatments

External beam radiotherapy was delivered in fractions of 1.8 Gy per day (total dose, 50.4 Gy). Patients received concomitant fluoropyrimidine-based chemotherapy administered in a bolus, via a continuous venous infusion, or via oral capecitabine. Local restaging was performed ≥ 4 weeks after the completion of pCRT and included pelvic MRI and proctoscopy. Surgery was performed using the TME technique, as described elsewhere,¹⁹ and was scheduled for 6 to 8 weeks after the completion of pCRT.

Histopathology

Using the protocol from Quirke et al,²⁰ the surgical specimen was evaluated by the same team of pathologists, and the findings were reported according to the American Joint Committee on Cancer postchemoradiotherapy tumor–node–metastasis (ypTNM) classification.²¹

Imaging Technique and Evaluation

MRI was performed with a 1.5-Tesla unit (Avanto; Siemens, Erlangen, Germany) with phased-array body coils. The patients assumed the supine position. Each series of images included the following: 1) sagittal, oblique coronal (parallel to the long axis of the rectal cancer), and oblique axial (perpendicular to the long axis of the rectal cancer) T2-weighted images, with a repetition time of 3790 to 5354 ms, an echo time of 95 ms, a 3- to 4-mm section thickness, a field of view of 320 \times 286 mm, and an image matrix of 320 \times 257 and 2) precontrast oblique axial, contrast-enhanced oblique coronal, and axial fat-suppressed T1-weighted images, with a repetition time of 562 ms, an echo time of 4.6 ms, a flip angle of 70°, a 3- to 4-mm section thickness, a field of view of 330 \times 289 mm, and a matrix of 320 \times 210. Contrast-enhanced T1-weighted images were obtained after 60 s of intravenous administration of

a gadolinium-based contrast material (0.2 mL/kg up to a maximum of 16 mL, flow rate 2.0–2.5 mL/s, Omniscan; GE Healthcare AS, Oslo, Norway), followed by a 20-mL saline flush.

All of the studies were reviewed by 2 independent radiologists with different levels of experience in reading MRIs. Observer 1 (F.P.) had 9 years of experience in interpreting abdominal and pelvic MRIs. Observer 2 (F.C.) was a specialist registrar with only very limited experience in reading rectal cancer MRIs (<1 year). The less-expert reader was first trained in reading rectal MRIs by an MRI pelvic reader with 5 years of experience (C.L.) and familiarized with the nodal staging criteria for rectal MRIs using cases that were not included in the current study.

Each radiologist knew that the patients had been referred for rectal cancer staging but was blinded of the other radiologist's findings and unaware of the final operative and histopathologic findings. All of the T2-weighted images were reviewed at a workstation and assessed for mesorectal LN number, size, and morphology. The short diameter of each LN was measured in the transverse imaging plane, which was angled exactly perpendicular to the long axis of the rectal tumor. The criteria used to assess LN morphology included the LN signal intensity (ie, heterogeneous or homogeneous) and border contour characteristics (ie, irregular or sharp).^{14,22} An LN with either an irregular border or a heterogeneous signal intensity was regarded as positive, and an LN was regarded as negative if a sharp border and homogeneous signal intensity were demonstrated. The prediction of LN status was assessed by calculating the sum of the measures of the short diameter of all mesorectal LNs in each patient in both the pre-pCRT and post-pCRT data sets to determine the pre-pCRT and post-pCRT LN global sizes and the Δ LN global size.

After the analysis of the pre-pCRT and post-pCRT MRI was completed, to assess the interobserver agreement, all of the images were reviewed together by the 2 observers to enable the matching of the individual LNs. The procedure was made possible by relating the size and position of each node to the rectal wall, mesorectal fascia, other LNs, and blood vessels. In this manner, lesion-by-lesion analysis of the mesorectal LNs could be performed with certainty. Taking histopathology as the reference standard, the above morphologic criteria of the matched LNs on the post-pCRT data sets were also used to predict ypN status. In an exploratory analysis, for the first 26 study patients, the Δ LN global size was also calculated based on the contrast-enhanced T1-weighted images.

Statistical Analysis

All of the continuous variables had nonnormal distributions (assessed with the Kolmogorov–Smirnov test).

Data were consecutively reported as medians (range) for continuous variables and numbers (and percentages) for categorical variables and compared using the Mann–Whitney (independent variables), Wilcoxon rank-sum test (dependent), and χ^2 (categorical) tests. The observer agreement regarding LN morphology and the degree of agreement between post-pCRT MRI and ypN stage were calculated using Cohen κ test.²³ Values between 0 and 0.20 corresponded with slight agreement, those between 0.21 and 0.40 with fair agreement, those between 0.41 and 0.60 with moderate agreement, those between 0.61 and 0.80 with substantial agreement, and those between 0.81 and 1.0 with near-perfect agreement.²⁴

The receiver operator characteristic curves were calculated using the trapezoidal rule and analyzed to compare the sensitivity and specificity of the various Δ LN global size estimates (observers 1 and 2), taking the absence of disease at histopathology as the outcome. For possible important cutoff values (reductions of 50%, 60%, and 70% vs baseline), the relative areas under the curve (AUCs), sensitivities, specificities, positive predictive values, and NPVs with 95% CIs (using the Wilson score CIs for a proportion) were reported. Similarly, the ability of the Δ LN global size to estimate the absence of disease in T2- vs T1-weighted images was compared using the AUCs for both observers. The AUCs were compared in agreement with the method described by DeLong et al.²⁵

A logistic regression analysis was run taking as outcome the presence/absence of disease and as exposure the Δ LN global size for both observers. The estimates for the Δ LN global size (reported as $\beta \pm$ SE, and OR with 95% CI was also adjusted for other factors potentially associated with the outcome, eg, age, sex, tumor location, and surgical procedure). Statistical significance was set at $p \leq 0.05$. The statistical analyses were carried out with SPSS 21.0.

RESULTS

Patients and Treatments

The demographic characteristics, tumor location, surgical procedures undergone, and histopathologic findings of the study group are summarized in Table 1. Of the 64 patients evaluated, 49 (76.5%) showed ypN0 status, and 8 (12.5%) had a complete pathologic response (ypT0N0).

LN Number and Size

The total LN counts for the pre-pCRT and post-pCRT MRIs were 365 and 147 for observer 1 and 541 and 387 for observer 2. pCRT significantly reduced LN number, size, and global size for both observers ($p < 0.0001$; Table 2). Although the individual LN size was not significantly

TABLE 1. Clinical and Pathological Features of Patients

Characteristic	Value
Age, median (range), y	63 (35–83)
Sex, n (%)	
Men	46 (71.8)
Women	18 (28.1)
Tumor location, n (%)	
Low rectum (<7 cm from anal verge)	34 (53.1)
Mid rectum (7–11 cm from anal verge)	30 (46.8)
Surgical procedure, n (%)	
Low anterior resection	48 (75)
Abdominoperineal resection	14 (21.8)
Rectal anterior resection	2 (3.1)
ypT stage, n (%)	
0	8 (12.5)
Tis	1 (1.5)
1	6 (9.3)
2	20 (31.2)
3	27 (42.1)
4	2 (3.1)
ypN stage, n (%)	
Negative	49 (76.5)
Positive	15 (23.4)
Interval from post-pCRT MRI to surgery, median (range), wk	6 (4–11)

ypTN = pathological staging after chemoradiotherapy; pCRT = preoperative chemoradiotherapy.

different between the 2 observers for pre-pCRT ($p = 0.85$) or post-pCRT MRI ($p = 0.74$), the LN global size measurement was significantly higher for observer 2 ($p < 0.0001$) on both examinations because he counted significantly more LNs ($p < 0.0001$) than observer 1 (Table 2).

After pCRT, LN number and size were significantly different between ypN0 and ypN+ patients for observer 1 ($p < 0.0001$). In contrast, these were not different for observer 2 ($p = 0.94$ and 0.71), who counted more LNs in the ypN0 group, likely misinterpreting structures with

TABLE 2. Comparison of Pre-pCRT and Post-pCRT MRI Results by LN Number and Size

Parameter	LN No.	LN size, mm	LN global size, mm
Observer 1, median (range)			
Pre-pCRT MRI	5 (1–15)	5 (2–19)	24.0 (2.0–93.0)
Post-pCRT MRI	2 (1–10)	3 (1–18)	8.5 (1.0–49.0)
<i>p</i>	<0.0001	<0.0001	<0.0001
Observer 2, median (range)			
Pre-pCRT MRI	8 (1–18)	4 (2–19)	38.5 (3.0–95.0)
Post-pCRT MRI	6 (1–15)	3 (1–19)	18.5 (2.0–60.0)
<i>p</i>	<0.0001	<0.0001	<0.0001
Pre-pCRT MRI, median (range)			
Observer 1	5 (1–15)	5 (2–19)	24.0 (2.0–93.0)
Observer 2	8 (1–18)	4 (2–19)	38.5 (3.0–95.0)
<i>p</i>	<0.0001	0.85	<0.0001
Post-pCRT MRI, median (range)			
Observer 1	2 (1–10)	3 (1–18)	8.5 (1.0–49.0)
Observer 2	6 (1–15)	3 (1–19)	18.5 (2.0–60.0)
<i>p</i>	<0.0001	0.74	<0.0001

pCRT = preoperative chemoradiotherapy; LN = lymph node.

similar sizes and morphologies, such as blood vessels or areas of fibrotic residue, as LNs (Table 3). On the contrary, the initial TNM stage (stage II vs III) did not affect the Δ LN global size for either observer (observer 1: $84.3\% \pm 20.0\%$ for stage II vs $68.5\% \pm 26.4\%$, $p = 0.07$; observer 2: $58.0\% \pm 31.6\%$ for stage II vs $53.8\% \pm 15.2\%$, $p = 0.51$). The analysis of LN number and size for ypN0 and ypN+ patients showed no significant difference between the 2 observers ($p > 0.30$), except in LN number for the ypN0 group ($p < 0.0001$), probably because pCRT changes in LN number were of a higher degree for the ypN0 group than for the ypN+ group, increasing the risk of misdiagnosis during local nodal assessment (Table 3).

The Δ LN global size performance, using various cut-off values for comparison with the final histopathologic evaluation, is shown in Table 4. With a cutoff of 70%, the NPV rate was 97.1% (95% CI, 82.9%–99.8%) for observer 1, corresponding to 1 false-negative case (Fig. 1), and 100% (95% CI, 62.9%–100%) for observer 2. The AUCs for the 2 observers were 0.90 (95% CI, 0.82–0.98; $p < 0.0001$) for observer 1 and 0.65 (95% CI, 0.50–0.79; $p = 0.08$) for observer 2.

Using a logistic regression analysis and taking as outcome the presence of disease, the Δ LN global size was associated with a decreased risk of having disease for observer 1 ($\beta = -0.09 \pm 0.02$; OR = 0.92; 95% CI, 0.88–0.96; $p < 0.0001$) but not for observer 2 ($\beta = -0.02 \pm 0.02$; OR = 0.98; 95% CI, 0.95–1.01; $p = 0.15$). Similar findings were evident after adjusting for age, sex, tumor location, and surgical procedure (observer 1: $\beta = -0.10 \pm 0.03$; OR = 0.91; 95% CI, 0.86–0.96, $p < 0.0001$; observer 2: $\beta = -0.03 \pm 0.02$; OR = 0.97; 95% CI, 0.93–1.01; $p = 0.08$).

LN Morphology Criteria

Using pre-pCRT and post-pCRT MRI, the 2 independent observers evaluated the same 197 and 92 LNs for signal intensity and border characteristics on T2-weighted MRI. The interobserver agreement (κ value) for assigning nodes into positive or negative groups based on this model was poor for both the pre-pCRT ($\kappa = 0.00 \pm 0.03$ (95% CI, 0.00–0.06); $p = 0.80$ for signal and 0.05 ± 0.05 (95% CI, 0.00–0.10); $p = 0.54$ for borders) and post-pCRT MRI (0.30 ± 0.25 (95% CI, 0.00–0.80); $p = 0.15$ for signals and 0.05 ± 0.15 (95% CI, 0.00–0.35); $p = 0.90$ for borders). The κ values tended to be higher for LNs ≥ 5 mm for determining the signal intensity and border characteristics only before pCRT ($\kappa = 0.50 \pm 0.15$ (95% CI, 0.20–0.80), $p = 0.002$ for signal and $\kappa = 0.36 \pm 0.16$ (95% CI, 0.04–0.68), $p = 0.04$ for borders). LN morphology after pCRT did not correlate with histopathology for either observer (all $p > 0.05$).

Contrast-Enhanced MRI

To investigate whether contrast-enhanced T1-weighted images were valuable for the preoperative assessment of

TABLE 3. Comparison of Post-pCRT MRI and Pathologic Results by N Classification

Parameter	LN No.	LN size, mm	LN global size, mm	ΔLN global size, %
Observer 1, median (range)				
ypN0	1 (1–9)	3 (1–7)	6 (1–49)	87.5 (22.2–100)
ypN+	4 (1–10)	4 (2–18)	21 (5–43)	38.8 (16.6–82.0)
<i>p</i>	<0.0001	<0.0001	<0.0001	<0.0001
Observer 2, median (range)				
ypN0	6 (1–15)	3 (1–8)	17 (2–60)	58.8 (9.0–100)
ypN+	5 (3–10)	4 (1–19)	22 (10–54)	50.9 (13.0–66.6)
<i>p</i>	0.94	0.71	0.08	0.45
ypN0, median (range)				
Observer 1	1 (1–9)	3 (1–8)	6 (1–49)	87.5 (22.2–100)
Observer 2	6 (1–15)	4 (2–8)	17 (2–60)	58.8 (9.0–100)
<i>p</i>	<0.0001	0.48	<0.0001	<0.0001
ypN+, median (range)				
Observer 1	4 (1–10)	4 (2–18)	21 (5–43)	38.8 (16.6–82)
Observer 2	5 (3–10)	4 (1–19)	22 (10–54)	50.9 (13.0–66.6)
<i>p</i>	0.84	0.37	0.86	0.28

pCRT = preoperative chemoradiotherapy; ypN = pathological staging after chemoradiotherapy; ΔLN global size = lymph node global size reduction rate.

N stage in pCRT patients, an exploratory analysis of the first 25 study patients was performed. The AUC values of the T2-weighted MRI images and contrast-enhanced T1-weighted MRI images were 0.90 (95% CI, 0.82–0.98; $p < 0.0001$) and 0.60 (95% CI, 0.36–0.84; $p = 0.43$) for observer 1 and 0.65 (95% CI, 0.50–0.79; $p = 0.55$) and 0.57 (95% CI, 0.34–0.81; $p = 0.55$) for observer 2. The diagnostic performance (AUC) of contrast-enhanced T1-weighted MRI was worse than T2-weighted MRI for both observers.

DISCUSSION

The crucial issue in selecting LARC patients for less invasive treatment approaches that do not include LN removal is the identification of disease without malignant LNs at the time of the procedure. The main goal of this study was to evaluate the performance of MRI in predicting ypN0 status when restaging LARC patients, using a patient-by-patient analysis. Although studies of LNs that involve a lesion-by-lesion comparison between MRI and histology

are important in establishing the diagnostic imaging criteria, the prediction of the nodal disease on a per-patient basis is more clinically relevant in terms of orienting treatment decisions, regardless of the number of positive LNs.

Using the dimensional criterion, MRI studies of the prediction of ypN staging report contradictory findings when analysis is performed on a per-patient basis, with sensitivity and specificity values of 33% to 83% and 68% to 100% and NPVs of 78% to 96%,^{15,18,26,27} likely because there was a substantial overlap in the size of individual benign and malignant LNs in irradiated LARC. Although the performance of the size criterion after pCRT seems to be better than its performance for initial staging,^{14,28} these findings call into question the validity of the dimensional criterion in the assessment of individual LN status.

Our findings show that the most accurate predictor of negative LN status was a ΔLN global size cutoff value of 70% when comparing MRI images before and after pCRT, with NPV values of 97% and 100% for the more- (observer 1) and less- (observer 2) experienced readers.

TABLE 4. Prediction of ypN Status by Various Cutoff Values for ΔLN Global Size After pCRT for Rectal Cancer

Parameter	ΔLN global size cutoff					
	Observer 1			Observer 2		
	50	60	70	50	60	70
True positive (n)	11	12	14	6	12	15
True negative (n)	45	40	33	33	29	9
False positive (n)	4	9	16	16	20	40
False negative (n)	4	3	1	9	3	0
Sensitivity % (95% CI)	73.3 (48.0–89.1)	80.0 (54.8–93.0)	93.3 (70.2–98.8)	40.0 (19.8–64.3)	80.0 (54.8–93.0)	100 (79.6–100)
Specificity % (95% CI)	91.8 (80.8–96.8)	81.6 (68.9–90.0)	67.3 (53.3–78.8)	67.3 (53.3–78.8)	59.2 (45.2–71.8)	18.4 (9.8–31.4)
NPV % (95% CI)	91.8 (79.5–97.3)	93.0 (79.9–98.2)	97.1 (82.9–99.8)	78.6 (66.3–89.2)	90.6 (73.8–97.6)	100 (62.9–100)
PPV % (95% CI)	73.3 (44.8–91.1)	57.1 (34.4–77.4)	46.7 (34.6–71.2)	27.3 (11.6–50.4)	37.5 (21.7–56.3)	27.3 (16.5–41.1)
AUC (95% CI)		0.90 (0.82–0.98)			0.65 (0.50–0.79)	

pCRT = preoperative chemoradiotherapy; ypN = pathological lymph node staging after chemoradiotherapy; ΔLN global size = lymph node global size reduction rate; NPV = negative predictive value; PPV = positive predictive value; AUC = area under the curve.

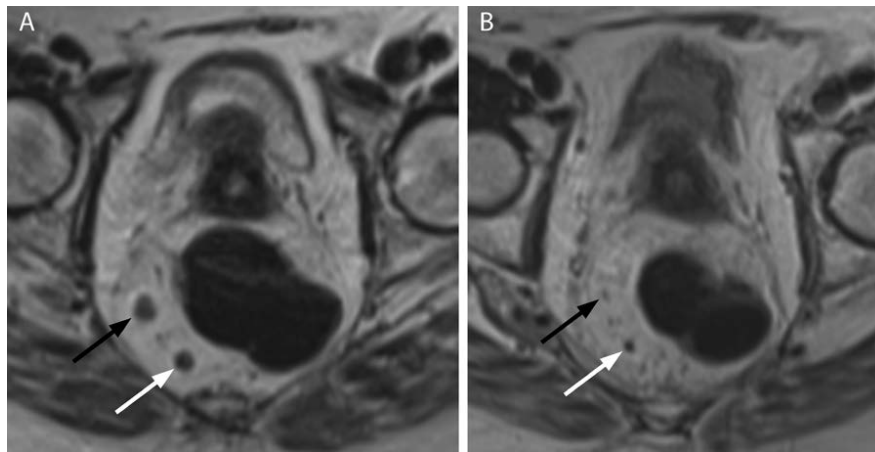


FIGURE 1. Transverse T2-weighted images of a rectal cancer before (A) and after (B) chemoradiotherapy (CRT). A, The preoperative CRT image shows 2 lymph nodes (arrows). Another lymph node was present at a different level (not shown). B, After CRT, 1 lymph node changed to an ill-defined structure (black arrow), which was interpreted as fibrosis by observer 1 and as residual lymph node by observer 2 (similar to the lymph node not shown). Micrometastases were detected in 2 of the 3 lymph nodes retrieved for histopathologic analysis.

With a high rate of ypN0 patients after CRT of 76.5%, the high sensitivity leads to an NPV of $\approx 100\%$, irrespective of the experience of the radiologist.

Unexpectedly, node signal intensity and border contour characteristics were unreliable criteria for the detection of negative LNs after pCRT, likely because the judgment of such characteristics in small LNs is challenging, even for the experienced observer. In addition, the interobserver variability in assigning nodes into positive or negative groups based on this model was considerable and highly dependent on the experience of the observers. An additional finding of the present study was that the addition of static gadolinium-enhanced T1-weighted images does not add information to T2-weighted images for the assessment of LN status in irradiated LARC. These findings suggest that gadolinium-enhanced MRI sequences can therefore be omitted from the standard MRI protocol, thus reducing acquisition time and examination costs and avoiding the potential development of any contrast media-related risk. The use of dynamic gadolinium-enhanced sequences has been reported to be useful in the prediction of LN involvement after pCRT for LARC by enabling the assessment of the characteristics of arterial phase enhancement.²⁹ However, it remains uncertain whether these techniques would offer any help for LNs measuring ≤ 3 mm.

When considering a rectum-sparing approach in patients with major or complete clinical response, the NPV value is the most relevant piece of information because it would be much worse to leave the mesorectum in situ, as happens when a transanal local excision is performed or a wait-and-see policy is adopted in patients with positive LNs than it would be to remove it (TME) in patients with negative nodes. From this point of view, it is important to know that LNs that are negative on MRI are also negative on histopathologic testing. For this reason, the specific Δ LN global size cutoff value of 70% was chosen to

optimize the NPV. With this cutoff the NPV was 97.0% and 100% and sensitivity 93.3% and 100% for observers 1 and 2.

In 1 study of nodal restaging after pCRT,¹³ the authors compared pre-pCRT and post-pCRT MRI and found that a decrease in the size of individual LNs of $\geq 70\%$ indicates ypN0 status in 100% of cases. This remarkable result does not provide information on the preoperative staging of each patient, which has practical clinical relevance in planning a less-invasive surgery. To our knowledge, our study is the first to calculate the global LN size and demonstrate a significant association with ypN0 status in patients with a nodal global size reduction rate of $\geq 70\%$.

The message that radiologists with very different experience levels can reach similarly good results when predicting ypN0 status is encouraging and makes this criterion easily applicable in clinical practice. Nevertheless, hand measurement and comparison of < 19 LNs in a patient are issues of concern. A computer-aided procedure for automated measuring and matching of LNs imaged in 2 serial clinical MRI studies might provide support for broad application of our type of analysis in the future.

The specificities of 67.3% and 18.4%, with positive predictive value values of only 46.7% and 27.3% for observers 1 and 2, indicate node overstaging. One explanation for overstaging is that small blood vessels or small areas of fibrosis in the mesorectum can easily be misinterpreted as small LNs.²⁸ Typically, the less experienced observer chose a safer approach in these cases, and his behavior led to more overstaging. Consequently, we were able to obtain a good overall performance for observer 1 (AUC of 0.90) but a poor performance for observer 2 (AUC of 0.65). The limitations of this study were the small sample size, its retrospective nature, and the high rate of negative nodes after long-course pCRT, which resulted in a decrease in false-negative findings.

CONCLUSION

We found that, whereas individual nodal size and morphologic MRI criteria are poor predictors of LN status in patients with irradiated LARC, the MRI measurement of global LN size reduction rate results in a reproducible NPV close to 100%, with a high sensitivity. The ability of this criterion to accurately identify ypN0 patients after pCRT may improve the selection of candidates for rectum-sparing approaches. This study also suggests that, in determining LN status after pCRT, gadolinium-enhanced MRI sequences do not add any relevant information as compared with unenhanced MRI. Because of the retrospective nature of the study and the small sample size, large and prospective studies are required to validate the findings of the present study.

ACKNOWLEDGMENTS

The authors thank Salvatore Pucciarelli, M.D., who had a fundamental role in the conception and design of this study, analysis and interpretation of data, and final revision of the article.

REFERENCES

- Benson AB 3rd, Venook AP, Bekaii-Saab T, et al. NCCN Guidelines Insights: rectal cancer, version 2.2015. *J Natl Compr Canc Netw*. 2015;13:719–728.
- Sauer R, Becker H, Hohenberger W, et al.; German Rectal Cancer Study Group. Preoperative versus postoperative chemoradiotherapy for rectal cancer. *N Engl J Med*. 2004;351:1731–1740.
- Agarwal A, Chang GJ, Hu CY, et al. Quantified pathologic response assessed as residual tumor burden is a predictor of recurrence-free survival in patients with rectal cancer who undergo resection after neoadjuvant chemoradiotherapy. *Cancer*. 2013;119:4231–4241.
- Park IJ, You YN, Agarwal A, et al. Neoadjuvant treatment response as an early response indicator for patients with rectal cancer. *J Clin Oncol*. 2012;30:1770–1776.
- Giandomenico F, Gavaruzzi T, Lotto L, et al. Quality of life after surgery for rectal cancer: a systematic review of comparisons with the general population. *Expert Rev Gastroenterol Hepatol*. 2015;9:1227–1242.
- Bujko K, Richter P, Smith FM, et al. Preoperative radiotherapy and local excision of rectal cancer with immediate radical reoperation for poor responders: a prospective multicentre study. *Radiother Oncol*. 2013;106:198–205.
- Pucciarelli S, De Paoli A, Guerrieri M, et al. Local excision after preoperative chemoradiotherapy for rectal cancer: results of a multicenter phase II clinical trial. *Dis Colon Rectum*. 2013;56:1349–1356.
- Habr-Gama A, Gama-Rodrigues J, São Julião GP, et al. Local recurrence after complete clinical response and watch and wait in rectal cancer after neoadjuvant chemoradiation: impact of salvage therapy on local disease control. *Int J Radiat Oncol Biol Phys*. 2014;88:822–828.
- Park IJ, You YN, Skibber JM, et al. Comparative analysis of lymph node metastases in patients with ypT0-2 rectal cancers after neoadjuvant chemoradiotherapy. *Dis Colon Rectum*. 2013;56:135–141.
- Maas M, Nelemans PJ, Valentini V, et al. Long-term outcome in patients with a pathological complete response after chemoradiation for rectal cancer: a pooled analysis of individual patient data. *Lancet Oncol*. 2010;11:835–844.
- Pucciarelli S, Capirci C, Emanuele U, et al. Relationship between pathologic T-stage and nodal metastasis after preoperative chemoradiotherapy for locally advanced rectal cancer. *Ann Surg Oncol*. 2005;12:111–116.
- Debove C, Guedj N, Tribillon E, Maggiori L, Zappa M, Panis Y. Local excision of low rectal cancer treated by chemoradiotherapy: is it safe for all patients with suspicion of complete tumor response? *Int J Colorectal Dis*. 2016;31:853–860.
- Heijnen LA, Maas M, Beets-Tan RG, et al. Nodal staging in rectal cancer: why is restaging after chemoradiation more accurate than primary nodal staging? *Int J Colorectal Dis*. 2016;31:1157–1162.
- An C, Huh H, Han KH, et al. Use of preoperative MRI to select candidates for local excision of MRI-staged T1 and T2 rectal cancer: can MRI select patients with N0 tumors? *Dis Colon Rectum*. 2015;58:923–930.
- Park JS, Jang YJ, Choi GS, et al. Accuracy of preoperative MRI in predicting pathology stage in rectal cancers: node-for-node matched histopathology validation of MRI features. *Dis Colon Rectum*. 2014;57:32–38.
- Zhou J, Zhan S, Zhu Q, et al. Prediction of nodal involvement in primary rectal carcinoma without invasion to pelvic structures: accuracy of preoperative CT, MR, and DWIBS assessments relative to histopathologic findings. *PLoS One*. 2014;9:e92779.
- Suppiah A, Hunter IA, Cowley J, et al. Magnetic resonance imaging accuracy in assessing tumour down-staging following chemoradiation in rectal cancer. *Colorectal Dis*. 2009;11:249–253.
- Perez RO, Pereira DD, Proscurshim I, et al. Lymph node size in rectal cancer following neoadjuvant chemoradiation: can we rely on radiologic nodal staging after chemoradiation? *Dis Colon Rectum*. 2009;52:1278–1284.
- Pucciarelli S, Friso ML, Toppán P, et al. Preoperative combined radiotherapy and chemotherapy for middle and lower rectal cancer: preliminary results. *Ann Surg Oncol*. 2000;7:38–44.
- Quirke P, Durdey P, Dixon MF, Williams NS. Local recurrence of rectal adenocarcinoma due to inadequate surgical resection: histopathological study of lateral tumour spread and surgical excision. *Lancet*. 1986;2:996–999.
- Colon and rectum. In: Edge SB, Byrd DR, Compton CC, Fritz AG, Greene FL, Trotti AE, eds. *AJCC Cancer Staging Manual*. 7th ed. New York, NY: Springer; 2010:143–164
- Patel UB, Blomqvist LK, Taylor F, et al. MRI after treatment of locally advanced rectal cancer: how to report tumor response—the MERCURY experience. *AJR Am J Roentgenol*. 2012;199:W486–W495.
- Cohen J. Weighted kappa: nominal scale agreement with provision for scaled disagreement or partial credit. *Psychol Bull*. 1968;70:213–220.
- Landis JR, Koch GG. The measurement of observer agreement for categorical data. *Biometrics*. 1977;33:159–174.

25. DeLong ER, DeLong DM, Clarke-Pearson DL. Comparing the areas under two or more correlated receiver operating characteristic curves: a nonparametric approach. *Biometrics*. 1988;44:837–845.
26. Maretto I, Pommeri F, Pucciarelli S, et al. The potential of restaging in the prediction of pathologic response after preoperative chemoradiotherapy for rectal cancer. *Ann Surg Oncol*. 2007;14:455–461.
27. Pommeri F, Pucciarelli S, Maretto I, et al. Prospective assessment of imaging after preoperative chemoradiotherapy for rectal cancer. *Surgery*. 2011;149:56–64.
28. Lahaye MJ, Beets GL, Engelen SM, et al. Locally advanced rectal cancer: MR imaging for restaging after neoadjuvant radiation therapy with concomitant chemotherapy—part II: what are the criteria to predict involved lymph nodes? *Radiology*. 2009;252:81–91.
29. Alberda WJ, Dassen HP, Dwarkasing RS, et al. Prediction of tumor stage and lymph node involvement with dynamic contrast-enhanced MRI after chemoradiotherapy for locally advanced rectal cancer. *Int J Colorectal Dis*. 2013;28:573–580.